# scientific reports



# **OPEN** Topographic analysis of retinal and choroidal vascular displacements after macular hole surgery

Areum Jeong<sup>1,2</sup>, Hyeonqjun Park<sup>1,2</sup>, Kyunqmin Lee<sup>3</sup>, Sanq Hyun Park<sup>3</sup> & Min Saqong<sup>1,2⊠</sup>

It has been reported that the retinal vessel and macular region of the retina are displaced after macular hole (MH) surgery. However, there is no detailed information for correlations between retinal and choroidal displacements. We obtained optical coherence tomography angiography (OCTA) and en-face optical coherence tomography (OCT) images from 24 eyes to measure the retinal and choroidal vascular displacement before and after surgery. These images were merged into infrared images using blood vessel patterns. The same vascular bifurcation points were automatically selected for each follow-up image, and the displacements of the bifurcation points were analyzed as a vector unit for prespecified grid regions in a semi-automated fashion. The results showed displacements of the choroidal intermediate vessels and retinal vessels following MH surgery (p = 0.002, p < 0.001). The topographic changes showed inferior, nasal, and centripetal displacement of the retina and inferiorly displaced choroid. The ILM peeling size and basal MH size were significantly associated with the retinal displacement (p < 0.001 and p = 0.010). Additionally, changes in the amount of the choroidal displacement were significantly correlated with that of the retinal displacements (p = 0.002). Clinicians should keep in mind that there might be topographic discrepancies of the displacement between retina and choroid when analyzing them following surgery.

Macular hole (MH) can be successfully closed by vitrectomy with internal limiting membrane (ILM) peeling and gas tamponade<sup>1</sup>. Gass et al. postulated that the principal initial step in the closure of MH is a glial proliferation and centripetal traction of the fovea, resulting from an increase in Muller cells above the fovea<sup>2</sup>. However, recent research has demonstrated that additional factors, such as the postoperative asymmetric elongation of foveal tissue and foveal displacement to optic disc might play a role<sup>3,4</sup>. Technical modifications have been made to reduce postoperative metamorphopsia. Broad ILM peeling results in enhanced glial cell stimulation and reduced residual ILM contraction minimizes centrifugal movements<sup>5,6</sup>. The exact asymmetrical displacements have still not been determined and more detailed data on the displacement over the whole macula could provide further information. Previous studies suggested several methods to measure retinal displacement. Rodrigues IA et al. conducted analysis of fundus autofluorescence (FAF) to detect signs of retinal displacement and took measurements of vertical interarcade distance, fovea to disc margin, and perimacular area<sup>7</sup>. Another study analyzed the displacement of the retinal vessels after surgical closure of idiopathic macular hole by calculating vector values of four vascular bifurcation points<sup>8</sup>.

OCTA has the advantages of being able to obtain the vasculatures of deeper layers as well as superficial retinal vessels because it could provide the depth information non-invasively and repeatedly in short intervals<sup>9</sup>. One study compared the postoperative foveal avascular zone (FAZ) and papillofoveal distance to their baseline areas on OCTA images, to ascertain if the centripetal displacement of capillaries in the macular region after vitrectomy is a result of ILM peeling<sup>10</sup>. However, only the superficial layer was used to demonstrate the changes in macular blood vessels. Recent study using 3×3 mm<sup>2</sup> en-face images showed that choroidal displacement after MH surgery<sup>11</sup>. However, 3 × 3 mm<sup>2</sup> images with narrow field of view could not represent the entire retinal or choroid and there is no detailed information for topographic correlations between retinal and choroidal displacements.

<sup>1</sup>Department of Ophthalmology, Yeungnam University College of Medicine, #170 Hyunchungro, Nam-Gu, Daegu 42415, South Korea. <sup>2</sup>Yeungnam Eye Center, Yeungnam University Hospital, Daegu, South Korea. <sup>3</sup>Department of Robotic Engineering, DGIST, #333, Techno Jungang-Daero, Dalseong-Gun, Daegu, South Korea. <sup>™</sup>email: msagong@yu.ac.kr

Therefore, this study was conducted to investigate the retinal and choroidal changes after MH surgery using vascular bifurcation points on en-face OCT and OCTA images, and to analyze related factors.

#### Results

#### Demographic and clinical data of patients

A total of 24 eyes from 24 participants were included, consisting of 6 males (25%) and 18 females (75%). The mean age of the subjects was  $63.96\pm10.26$ . The mean BCVA was  $0.828\pm0.270$  logMAR units preoperatively, which improved to  $0.172\pm0.169$  logMAR units at 6 months postoperatively. There were 3 patients with stage 2 MH, 13 patients with stage 3 MH, and 8 patients with stage 4 MH. The mean basal MH size was  $820.29\pm346.17$  µm, while the mean minimum MH size was  $412.79\pm141.53$  µm. The Mean ILM peeling size was  $3.50\pm0.42$  disc diameter. 6 patients (25%) underwent vitrectomy only and 18 patients (75%) underwent vitrectomy and cataract surgery as a combined procedure. As the gas tamponade agent, SF6 gas was used in 23 eyes (95.8%) and C3F8 gas was used in 1 eye (4.2%). Horizontal and vertical m-chart score were  $0.29\pm0.33$  and  $0.39\pm0.39$  preoperatively. They were  $0.07\pm0.13$  and  $0.16\pm0.26$  at 6 months postoperatively (Table 1).

# Retinal and choroidal displacement

Six months after surgery, the mean retinal displacement was  $62.4 \, \mu m$  at  $-5.7^{\circ}$  and the mean choroidal displacement was  $22.8 \, \mu m$  at  $-34.4^{\circ}$ . Overall, the retina showed greater asymmetrical displacement than the choroid, and although the choroidal displacement was less, it showed consistent displacement toward inferonasal side (Table 2).

When analyzed by dividing into inner ring and outer ring, changes in distance of retinal and choroidal displacement at 6 months were significantly different in all quadrants throughout the postoperative period (p < 0.001). The distance of retinal displacement was significantly greater than that of the choroid in both inner

	Total patients (24 eyes)
Age (years)	63.96 ± 10.26
Male/Female	6/18
OD/OS	12/12
Preoperative visual acuity (logMAR)	$0.828 \pm 0.270$
6-month postoperative visual acuity (logMAR)	0.172±0.169
MH stage 2:3:4	3:13:8
Basal MH size (µm)	820.29 ± 346.17
Minimum MH size (μm)	412.79 ± 141.53
ILM peeling size (DD)	$3.50 \pm 0.42$
PPV + PEA + IOL/PPV (eyes)	18/6
Gas tamponade (C3F8 : SF6)	1:23
Preoperative horizontal M score	0.29 ± 0.33
Preoperative vertical M score	0.39 ± 0.39
6-month postoperative horizontal M score	0.07 ± 0.13
6-month postoperative vertical M score	0.16±0.26

**Table 1.** Demographic and clinical characteristics of the pateints. PPV, Pars Plana Vitrectomy; PEA, Phacoemulsification; C3F8, perfluoropropane; SF6, Sulfur hexafluoride. Values are presented as mean ± standard deviation.

		Sector	Т	IT	I	IN	N	SN	S	ST
Retina	Inner ring	Distance (µm)	276.5	217.2	113.5	54.3	86.7	121.3	187.6	207.2
		Angle (°)	-6.7	13.2	29.2	41.9	5.1	-44.7	- 32.7	-14.1
	Outer ring	Distance (µm)	164.8	147.7	89.6	16.7	19.8	98.2	167.5	181.4
		Angle (°)	-4.6	4.9	32.7	42.2	7.5	-37.1	-34.4	-7.9
Choroid	Inner ring	Distance (µm)	55.2	61.7	43.6	52.8	61.1	67.4	76.7	69.4
		Angle (°)	-25.8	-34.3	-45.7	-40.2	-33.5	-36.1	-46.2	-30.4
	Outer ring	Distance (µm)	57.6	65.3	55.5	62.7	60.4	74.4	83.1	78.2
		Angle (°)	-26.9	-31.4	-47.1	-42.5	- 34.2	-37.8	-48.3	- 32.6

**Table 2.** Distance and angle of mean retinal and choroidal displacement in each Sect. 6 month after closure of macular hole. T, temporal; IT, infero-temporal; I, inferior; IN, infero-nasal; N, nasal; SN, supero-nasal; S, superior; ST, supero-temporal.

and outer ring (p < 0.001). The displacement of each segment by time period was shown in Supplementary Figure S1.

Changes in the angle of the retinal and choroidal displacement over time showed significant changes in all segments throughout the postoperative period (p < 0.001). Most of the retinal and choroidal displacement occurred within 1 month and maintained for 6 months after surgery (see Supplementary Fig. S2 online).

When we illustrate these displacements using en face OCT images, the retina was displaced centripetally, nasally, and slightly inferiorly, with the displacement being more pronounced in the temporal segment. The choroid was consistently displaced in the inferonasal direction (Fig. 1).

## Association between displacement and other variables

In a multivariate regression analysis, the basal size of the MH and the size of ILM peeling were identified as significant determinants influencing retinal displacement (p = 0.010 and p < 0.001) (Table 3). In the analysis of factors related to choroidal displacement, retinal displacement was the only related factor (p = 0.002) (Table 4).

# Relationship between retina & choroidal displacement

Taken as a whole, changes in the distance of choroidal displacement were significantly correlated with that of retinal displacements (p = 0.001). A stronger correlation was observed in the inner ring than in the outer ring (r = 0.386, p = 0.045) and the temporal sector showed the highest correlation among 8 segments (r = 0.417, p = 0.003).

(see Supplementary Fig. S3 online). Changes in the angle of choroidal displacement were not correlated with that of retinal displacements in the whole macula. However, the correlation was observed in the inner ring (r = 0.271, p = 0.047) and the superior sector showed the highest correlation among 8 segments (r = 0.324, p = 0.002) (see Supplementary Fig. S4 online).

Retina

# Choroid

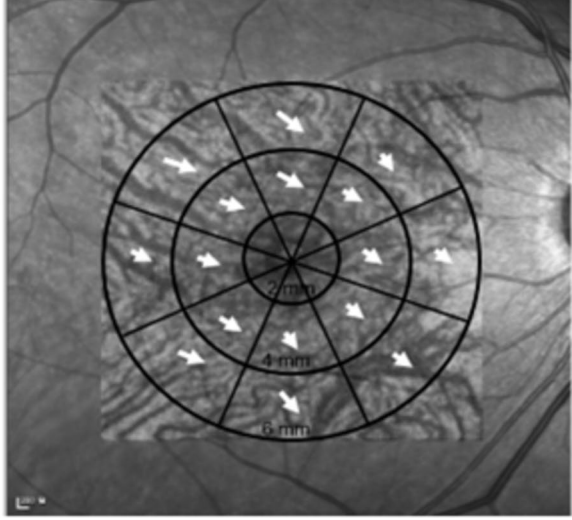


Figure 1. Schematic images of retinal and choroid displacement after macular hole surgery.

	Univariate		Multivariate		
	β	P value	β	P value	
Age	-0.259	0.417			
Gender	0.142	0.610			
Preoperative BCVA	0.454	0.487			
6-month postoperative BCVA	0.495	0.364			
M-score	0.375	0.152			
Basal MH size	0.598	0.025	0.612	0.010	
Minimum MH size	0.318	0.033			
ILM peeling size	0.656	0.002	0.672	< 0.001	
Type of surgery (vitrectomy or combined surgery)	0.109	0.656			
Type of gas (C3F8 or SF6)	0.168	0.497			

**Table 3.** Association between retinal displacement and other variables. BCVA, best corrected visual acuity; MH, macular hole; ILM, internal limiting membrane; C3F8, perfluoropropane; SF6, sulfur hexafluoride.

	Univariate		Multivariate		
	β	P value	β	P value	
Age	-0.095	0.398			
Gender	0.062	0.210			
Preoperative BCVA	0.406	0.640			
6-month postoperative BCVA	0.626	0.429			
M-score	0.497	0.226			
Basal MH size	0.521	0.103			
Minimum MH size	0.619	0.308			
ILM peeling size	0.775	0.072			
Type of surgery (vitrectomy or combined surgery)	0.653	0.503			
Type of gas (C3F8 or SF6)	0.159	0.834			
Changes in distance of retina	0.425	0.012	0.506	0.002	

**Table 4.** Association between choroidal displacement and other variables. BCVA, best corrected visual acuity; MH, macular hole; ILM, internal limiting membrane; C3F8, perfluoropropane; SF6, sulfur hexafluoride.

#### Discussion

This study showed that centripetal, inferior, and nasal displacement of the retina and inferonasally displaced choroid following MH surgery. Larger and more asymmetrical displacements were observed in the retina than in the choroid. In addition, Basal MH size and ILM peeling size were significantly correlated with the distance of the retinal displacement. Changes in distance of the choroidal displacement were significantly associated with that of the retinal displacements.

Under physiological conditions, the ILM pulls more on the fovea from the temporal side due to the absence of ILM at the optic disc. The ILM peeling could alter this balance, removing centrifugal forces<sup>4</sup>. Therefore, the process of MH closure causes centripetal displacement. In this study, larger displacement was noted in the inner ring than in the outer ring and the superior and inferior segments were displaced toward the horizontal raphe, which corroborate previous reports<sup>8</sup>. Moreover, the ILM peeling could lead to a loss of structural support of retina and retinal nerve fiber layer (RFNL). The nerve fibers consist mainly of microtubules, and depolymerization of microtubules may cause neuronal contractions. Because the nerve fibers are anchored to lamina cribrosa, contraction might move the retina toward the optic disc<sup>12</sup>. It is presumed that this contraction forced by RFNL displaced the retina nasally. Additionally, gas tamponade also might affect the retinal displacement. The buoyancy generated by the gas would be greatest in the superior quadrant causing a downward displacement of the retina<sup>13</sup>. Furthermore, the combined effects of nasal displacement and centripetal contraction forces could be observed in the temporal sector. In contrast, these forces might counteract each other in the nasal sector, leading to a mitigated effect. This interaction could explain the asymmetrical displacement of the temporal and nasal retina<sup>12</sup>.

Results of this study showed that the choroid was displaced inferonasally at all sectors following MH surgery and choroidal displacement was correlated with retinal displacement. As for the choroidal displacement, change in distance was less than that in the retina. This is partly due to the role of Muller cells, which are crucial in maintaining the structural integrity of the retina<sup>14</sup>. The sensory retina has a strong adherence to the RPE, a feature that actively facilitates fluid transport<sup>15</sup>. Consequently, when displacement occurs, the RPE layers are moved in conjunction with the inner retinal layer. It has been believed that the choriocapillaris does not typically undergo displacement from the RPE layer. Because the choriocapillaris lies adjacent to outermost layer of Bruch's membrane which is firmly bonded to the RPE, preventing the choriocapillaris from moving significantly. In previous studies using fundus autofluorescence (FAF) imaging, Shiragami et al. reported that the hyperfluorescent lines indicating displacement of inner retinal layer were observed in eyes with retinal attachment after retinal detachment surgery. However, Goto et al. reported that the hyperfluorescent line was not visible on FAF images after MH surgery, suggesting the inner retinal layer was displaced along with the RPE layer<sup>11,16</sup>. In this study, changes in distance of choroid were less than that in the retina. Choroid has the stroma containing extracellular tissue, elastic fiber, and collagen<sup>17</sup>. Thus, choroidal vessels are not adhesively connected in these layers and choriocapillaris layer, which might cause the gap in their displacement. This gap might lead to the difference in displacements between retina and choroid after the surgery. There is a more pronounced downward rotation of the angle in choroidal displacement when compared to the retina in all sectors. It appears that the downward movement of the retina due to the buoyancy of intraocular gas might have the greatest impact on the choroid. In addition, less downward displacement of the choroid in inner ring than outer ring and overall displacement of the choroid may be partly due to the centripetal and nasal displacement of retina.

There have been many reports about changes of the choroidal thickness or blood flow at the fovea after MH surgery. The choroid is displaced following the surgery, and the degree of the displacement in choroid is different from that in retina. This means that there are changes in the subfoveal choroid after surgery, which may cause differences in the measured area of the subfoveal choroid before and after surgery. Therefore, clinicians need to know that the displacement is different between the retina and choroid and it should be considered when evaluating the choroid after vitrectomy.

This study has several limitations. First, this study was a retrospective study with a limited number of participants and lacked comparative groups. Second, the analysis was based only on the blood vessel bifurcation

points, which could not fully reflect the entire retina or choroid. These aspects should be elucidated in future studies to analyze all pixels in the image. In addition, the relationship between postoperative displacement and more detailed functional outcome such as metamorphopsia was not evaluated.

In conclusion, the retina moves centripetally, nasally, and inferiorly, and the choroid moves inferonasally following MH surgery. ILM peeling size and basal MH size were significantly associated with the amount of the retinal displacement, whereas the amount of the choroidal displacement was correlated with the changes in distance of retina. Clinicians need to understand that after macular hole surgery, the retina and choroid show discrepancy in the amount of displacement but are correlated in its direction.

#### Methods

### **Ethical considerations**

The study was conducted in accordance with the Declaration of Helsinki, and the protocol was approved by the Institutional Review Board of Yeungnam University Hospital (IRB No.: 2023–12-050). Informed consent was waived because of the retrospective nature of the study. The need for informed consent is waived by the Ethics Committee of Yeungnam University Hospital and the subjects were provided an opportunity to opt out of the study.

# **Subjects**

A retrospective observational study of patients who underwent vitrectomy with ILM peeling for idiopathic MH between 2021 and 2022 was conducted. Patients who were able to follow up at least 6 months postoperatively were included in this study. All patients underwent follow up examinations at 1, 3 and 6 months postoperatively. Patients who had history of macular and other ocular diseases, high myopia of more than -6 diopters (D), previous retinal surgery, poor quality OCTA images (signal strength index  $\le 6$ ) were excluded.

All patients underwent a pars plana vitrectomy using 25-gauge instruments and phacoemulsification was combined concurrently according to the surgeon's discretion. All surgeries were performed by single experienced surgeon. The ILM was broadly and consistently peeled using indocyanine green, to the edge of the vascular arcade and close to the optic nerve papillary margin. After air-fluid exchange, intravitreal air was replaced with 20% sulfur hexafluoride (SF6) or 11% perfluoropropane (C3F8).

Clinical information including demographic data, comprehensive ophthalmic examination including best corrected visual acuity (BCVA), tonometry, OCT, and OCTA images throughout the entire clinical course were gathered at baseline, 1, 3 and 6 months after surgery.

### Image acquisition and analysis

The size of ILM removal was measured from surgical records. Minimum and basal MH size were obtained in vertical and horizontal planes on Spectralis® OCT (Heidelberg Engineering, Heidelberg, Germany) scans using embedded software caliper tool. We measured the minimum macular hole size as the minimum inner diameter between the macular hole edges, and the basal macular hole size as the diameter of the hole at the level of the RPE on OCT images <sup>18</sup> 6×6 mm<sup>2</sup> en face OCT and OCTA images were obtained using AngioVue (Optovue Inc., USA). Superficial capillary plexus (SCP) images were used to measure the displacements of the retina. Intermediate choroidal plexus images between 89 and 115 µm posterior to the retinal pigment epithelium (RPE) were obtained from the same area using OCT function to measure the displacement of the choroid. To precisely quantify the displacement of the retina and choroid, a fixed reference point was needed for each follow-up. Therefore, en face OCT and OCTA images were merged on infrared (IR) images with an expanded field of view, using the baseline optic nerve and the prominent blood vessels surrounding it as references. Using semi-automated algorithm, image registration was conducted on the OCTA and en face OCT images between the baseline and each followup<sup>19</sup> The proposed method consists of an encoder-decoder style network for predicting displacements and spatial transformers for making moved images using its predicted displacements. The algorithmToa transformed the moving image as well as its vesselness map generated by Frangi filtering and then compute the loss by comparing them with the target image and the corresponding vesselness maps (Fig. 2). After performing this registration, the dice similarity coefficient (DSC) showing the blood vessel registration rate was about 0.7. If the registration was not perfect, a manual correction was performed. The same vascular bifurcation points were automatically selected (Fig. 3A, B). If there were not enough automatic selected points, the number of points was increased by selecting them manually.

To assess the retina and choroidal displacement, the macula was partitioned via a customized grid of 16 sectors. The grid was composed of two rings each containing 8 sectors; inner ring: 2–4 mm diameter, outer ring: 4–6 mm diameter (Fig. 4). The displacements of the bifurcation points were analyzed as a vector unit composed of the mean displacement distance and direction angle. The angle was defined as 0° at the nasal horizontal direction, increasing in a counterclockwise direction in the right eye, clockwise direction in the left eye.

#### Statistical analysis

The one-way analysis of variance (ANOVA) with Bonferroni correction was used to evaluate the significance of the relationship between the displacements in the grid region and the chronological data. The association between retinal and choroidal displacements was calculated using the Spearman rank correlation coefficient. To ascertain the factors significantly linked to retinal and choroidal displacements, multivariate regression evaluations were conducted.

All statistical evaluations were conducted utilizing the Statistical Package for Social Sciences for Windows 21.0 (SPSS, Inc., Chicago, IL, USA). Two-tailed p-values less than 0.05 was considered to indicate statistical significance.

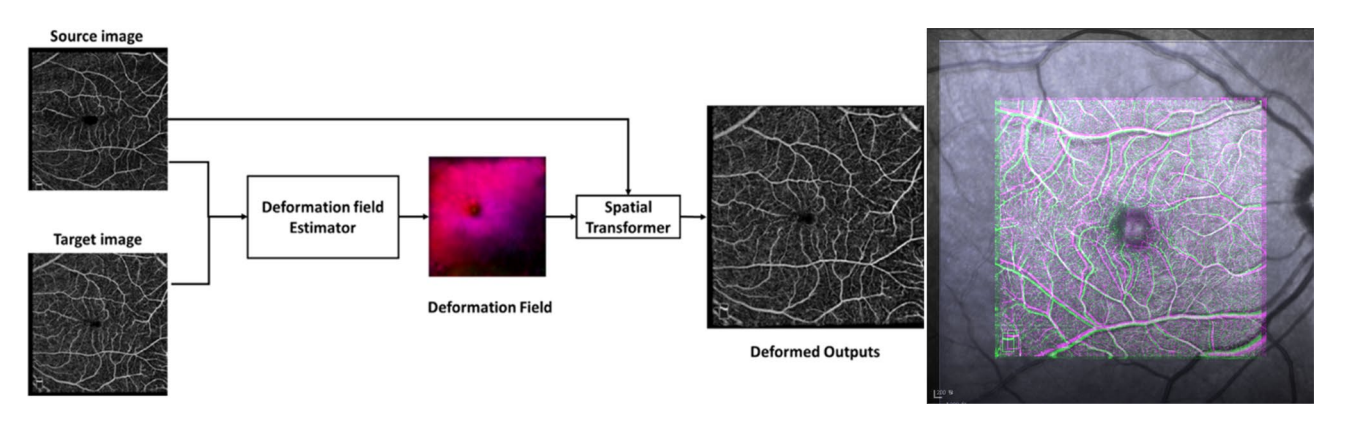


**Figure 2.** A deformation field was created by predicting pixel-level deformation between images using the deformation field estimator. The spatial transformer was trained to create a baseline and registered image from each input image using a deformation field.

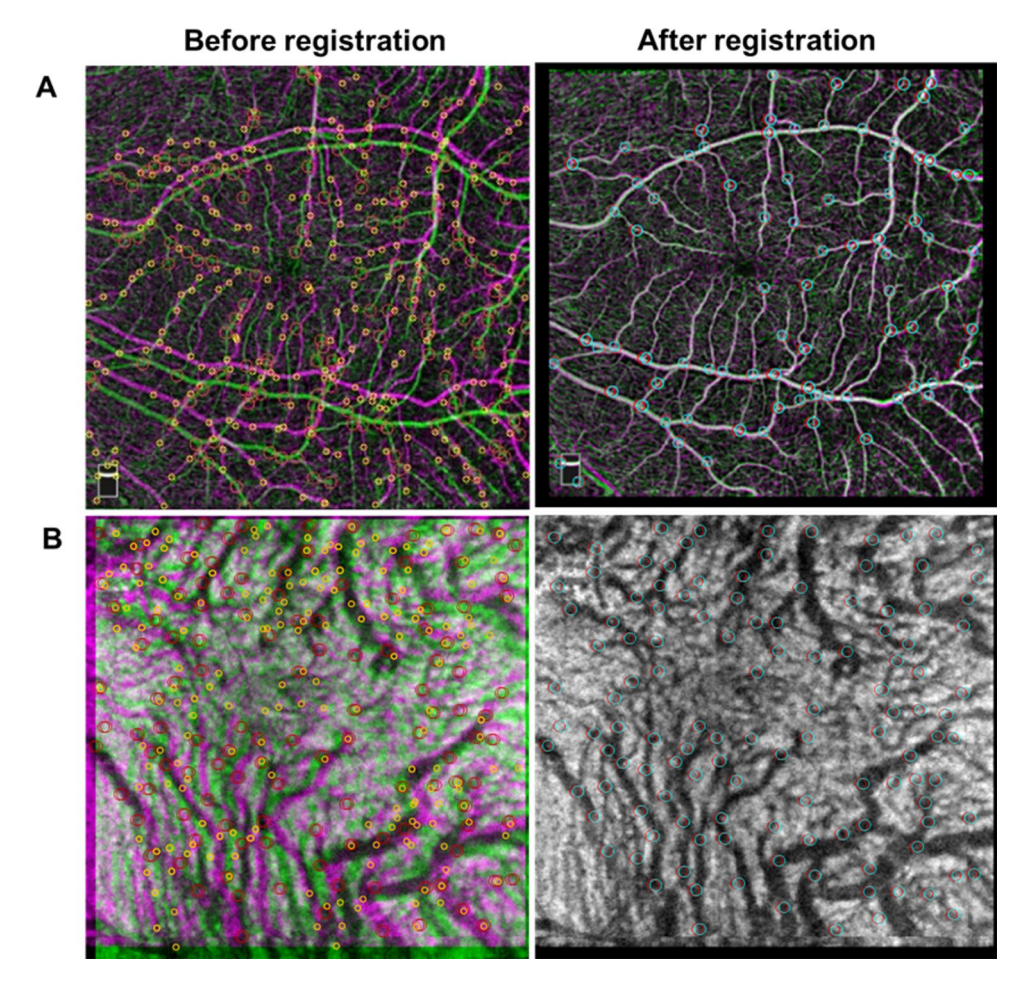


**Figure 3.** Superimposed image of pre-operative and post-operative image does not overlap perfectly. After the registration process, identical blood vessels are aligned. The same vascular bifurcation points were automatically selected in retina (**A**) and choroid (**B**).

**Figure 4.** The displacements of blood vessel bifurcations were analyzed as a vector unit comparing the images before and after registration and expressed by prespecified grid sectors. The grid was composed of two rings each containing 8 sectors; inner ring: 2–4 mm diameter, outer ring: 4–6 mm diameter.

# Data availability

The datasets used and/or analysed during the current study available from the corresponding author on reasonable request.

Received: 16 April 2024; Accepted: 14 August 2024

Published online: 16 August 2024

#### References

- 1. Garretson, B. R. et al. Vitrectomy for a symptomatic lamellar macular hole. Ophthalmology 115, 884-886 (2008).
- 2. Spaide, R. F. Closure of an outer lamellar macular hole by vitrectomy: hypothesis for one mechanism of macular hole formation. *Retina* **20**, 587–590 (2000).
- 3. Kim, J. H., Kang, S. W., Kim, S. J. & Ha, H. S. Asymmetric elongation of foveal tissue after macular hole surgery and its impact on metamorphopsia. *Ophthalmology* 119, 2133–2140 (2012).
- Kawano, K. et al. Displacement of foveal area toward optic disc after macular hole surgery with internal limiting membrane peeling. Eye 27, 871–877 (2013).
- Iezzi, R. & Kapoor, K. G. No face-down positioning and broad internal limiting membrane peeling in the surgical repair of idiopathic macular holes. Ophthalmology 120, 1998–2003 (2013).
- 6. Chatziralli, I. P., Theodossiadis, P. G. & Steel, D. H. Internal limiting membrane peeling in macular hole surgery; Why, when, and how?. Retina 38, 870–882 (2018).
- Rodrigues, I. A., Lee, E. J. & Williamson, T. H. Measurement of retinal displacement and metamorphopsia after epiretinal membrane or macular hole surgery. Retina 36, 695–702 (2016).
- 8. Pak, K. Y. et al. Topographic changes of the macula after closure of idiopathic macular hole. Retina 37, 667–672 (2017).
- 9. Khadamy, J. Optical coherence tomography angiography (OCTA) in ophthalmology: technology, pros, cons, and commercial prototypes. *JOJ Ophthal.* **2**(5), 555–598 (2017).
- 10. Kumagai, K., Ogino, N., Furukawa, M., Ooya, R. & Horie, E. Early centripetal displacements of capillaries in the macular region caused by internal limiting membrane peeling. *Clin. Ophthalmol.* 12, 755–763 (2018).
- 11. Goto, K. et al. Choroidal and retinal displacements after vitrectomy with internal limiting membrane peeling in eyes with idiopathic macular hole. Sci. Rep. 9(1), 17568 (2019).
- Ishida, M. et al. Retinal displacement toward the optic disc after internal limiting membrane peeling for idiopathic macular hole. Am. J. Ophthalmol. 157(5), 971–977 (2014).
- Akahori, T. et al. Macular displacement after vitrectomy in eyes with idiopathic macular hole determined by optical coherence tomography angiography. Am. J. Ophthalmol. 189, 111–121 (2018).
- 14. Franze, K. et al. Müller cells are living optical fibers in the vertebrate retina. Proc. Natl. Acad. Sci. 104(20), 8287-8292 (2007).
- 15. Stern, W. H., Ernest, J. T., Steinberg, R. H. & Miller, S. S. Interrelationships between the retinal pigment epithelium and the neurosensory retina. *Austr. J. Ophthalmol.* 8(4), 281–288 (1980).
- 16. Shiragami, C. *et al.* Unintentional displacement of the retina after standard vitrectomy for rhegmatogenous retinal detachment. *Ophthalmology* **117**(1), 86–92 (2010).
- 17. Heimann, K. The development of the choroid in man: Choroidal vascular system. Ophthal. Res. 3(5), 257-273 (1972).
- 18. Madi, H., Masri, I. & Steel, D. Optimal management of idiopathic macular holes. Clin. Ophthalmol. (Auckland N.Z) 10, 97–116 (2016).
- 19. Lee, G. M. et al. Unsupervised learning model for registration of multi-phase ultra-widefield fluorescein angiography. In *Medical Image Computing and Computer Assisted Intervention–MICCAI 2020: 23rd International Conference, Lima, Peru, October 4–8, 2020, Proceedings, Part III* (Vol. 23, p. 2020). Springer. (2020).

#### **Author contributions**

A.J. and H.P. performed the analysis, drafted the manuscript and designed the figures. K.L. and S.P designed the computational framework and analysed the data. M.S. devised the project, the main conceptual ideas and proof outline. All authors reviewed the manuscript.

### Competing interests

The authors declare no competing interests.

# Additional information

**Supplementary Information** The online version contains supplementary material available at https://doi.org/10.1038/s41598-024-70264-2.

**Correspondence** and requests for materials should be addressed to M.S.

**Reprints and permissions information** is available at www.nature.com/reprints.

**Publisher's note** Springer Nature remains neutral with regard to jurisdictional claims in published maps and institutional affiliations.

**Open Access** This article is licensed under a Creative Commons Attribution-NonCommercial-NoDerivatives 4.0 International License, which permits any non-commercial use, sharing, distribution and reproduction in any medium or format, as long as you give appropriate credit to the original author(s) and the source, provide a link to the Creative Commons licence, and indicate if you modified the licensed material. You do not have permission under this licence to share adapted material derived from this article or parts of it. The images or other third party material in this article are included in the article's Creative Commons licence, unless indicated otherwise in a credit line to the material. If material is not included in the article's Creative Commons licence and your intended use is not permitted by statutory regulation or exceeds the permitted use, you will need to obtain permission directly from the copyright holder. To view a copy of this licence, visit <a href="http://creativecommons.org/licenses/by-nc-nd/4.0/">http://creativecommons.org/licenses/by-nc-nd/4.0/</a>.

© The Author(s) 2024